Applied Energy 359 (2024) 122705

Contents lists available at ScienceDirect

Applied Energy

journal homepage: www.elsevier.com/locate/apenergy

Coordinated optimization of power-communication coupling networks for dispatching large-scale flexible loads to provide operating reserve

Liya Ma, Hongxun Hui *, Sheng Wang, Yonghua Song

State Key Laboratory of Internet of Things for Smart City, University of Macau, Macao, 999078, China
Department of Electrical and Computer Engineering, University of Macau, Macao, 999078, China

ARTICLE INFO

Keywords:
Power-communication coupling networks
Flexible loads
Coordinated optimization
Operating reserve

ABSTRACT

Increasing renewable energies bring more fluctuating power outputs, and make operating reserve become more important for maintaining the system balance. Regulating flexible loads to provide operating reserve has been widely accepted as a promising alternative, while the communication network will face enormous challenges due to the frequent data transmission and explosive data volume of large-scale distributed loads. To address this issue, this paper proposes a coordinated optimization framework of power-communication coupling networks for dispatching large-scale flexible loads to provide operating reserve. A power-communication equivalent model is established to couple the regulation power and transmitted data from flexible loads. The data nodes and branches in the communication network are formulated equivalently with power nodes and branches in the power network. On this basis, considering spatially and temporally dynamic power-communication coupling networks, the power flow and communication flow are coordinately optimized to minimize the regulation costs and communication costs. The proposed scheme is validated based on the 5-bus and 118-bus power-communication coupling networks. Numerical results illustrate that the coordinated optimization framework reallocates operating reserve capacities and decreases the regulation cost of power-communication coupling networks.

1. Introduction

1.1. Background

With the rapid growth of renewable generations, operating reserve becomes more important for maintaining the power system balance between supply-side and demand-side [1]. Operating reserve is usually provided by traditional generators, e.g., thermal power plants [2]. However, the operating reserve may be insufficient in the near future since traditional generators are phasing out gradually. To address this issue, providing operating reserves by regulating flexible loads has become a research hotspot around the world by utilizing the progressed information and communication technologies (ICTs) [3].

Generally, flexible loads include electric vehicles [4], heat pumps [5], air conditioners [6], et al. because (*i*) they account for a large share in power consumption and have huge regulation potential [7]; (*ii*) these flexible loads can store electrical energy or heat energy, and have small impacts on users during the regulation process [8]. Compared with a traditional generator, the regulation capacity from one flexible load is much smaller. Hence, large-scale flexible loads are aggregated to provide significant operating reserve capacity, which is named as load aggregator (LA). For example, Yang et al. [9] develop a resilient control strategy for aggregating distributed flexible loads to meet power system requirements even under cyber-attacks, which contributes to enhancing the security of operating reserve services provided by flexible loads. Zhang et al. [10] present data-driven offer strategies for LAs consisting of electric vehicles to provide regulation capacities. Wang et al. [11] propose a machine-learning technique to aggregate commercial air conditioners for the power system balance. Chen et al. [12] investigate an aggregation strategy of LAs with heating, ventilation, and air conditioning to provide regulation services.

To support the real-time regulation of large-scale flexible loads, multiple ICTs have been used in power systems, ranging from fiber optics to wireless and wireline networks [13]. For example, WiFi, ZigBee, and cellular communication networks are applied to control decentralized energy storage systems in [14]. 5G technology is investigated in [15] to utilize the fast communication speed to achieve quick regulation of flexible loads. Power line communication is utilized in [16] to realize the power dispatching of battery storage systems in microgrids.

* Corresponding author at: State Key Laboratory of Internet of Things for Smart City and Department of Electrical and Computer Engineering, University of Macau, Macao, 999078, China.
E-mail address: hongxunhui@um.edu.mo (H. Hui).

https://doi.org/10.1016/j.apenergy.2024.122705
Received 11 October 2023; Received in revised form 10 December 2023; Accepted 20 January 2024

Nomenclature

A. Abbreviations

ICT	Information and communication technology
ISO	Independent System Operator
LA	Load aggregator
PJM	Pennsylvania-Jersey-Maryland

B. Superscripts

A	Load aggregator
D	Dispatched power
F	Communication network
G	Generators
O	Original power
P	Power network
RN	Data-receiving node for specific branches
S	Data source node
SN	Data-sending node for specific branches

C. Sets

$\mathcal{A}$	Set of LAs
$\mathcal{G}$	Set of generators
$\mathcal{I}$	Set of data nodes
$\mathcal{K}$	Set of communication branches
$\mathcal{L}$	Set of power branches
$\mathcal{M}$	Set of electricity buses
$\mathcal{T}$	Set of time intervals

D. Indices

a	Index of LAs
g	Index of generators
i/j	Index of data nodes
k	Index of communication branches
l	Index of power branches
m	Index of electricity buses
t	Index of time intervals

E. Parameters

λ	Coefficient between the operating reserve capacity and data-sending volume
$\underline{\delta}/\overline{\delta}$	Minimum or maximum bus angle
$\underline{D}/\overline{D}$	Minimum or maximum transmission capability
$\underline{P}/\overline{P}$	Minimum or maximum power
a/b	Communication price parameters
B	Branch susceptance

F. Variables

α	Elements of Hessian matrix
δ	Bus angles
C	Costs
c	Cost functions
D	Data volume
H	Hessian matrix
P	Power
p	Communication prices
R	Operating reserve capacity

Fig. 1 shows a common dispatching structure of large-scale flexible loads, including the power network and communication network. In the power network, LAs aggregate multiple flexible loads and can be dispatched by the Independent System Operator (ISO) to provide operating reserve. Measurement devices (e.g., smart meters, phase measurement units, and control terminals) monitor the operation data of all the flexible loads [17], and upload these data to the ISO in the real-time. Specifically, in the communication network, the monitoring data is transmitted among base stations in the corresponding coverage areas and finally received by the ISO.

1.2. Challenges and motivations

The main challenges can be summarized as follows:

(1) *Frequent data transmission*: The data transmission process between ISO and units in Fig. 2 is necessary in each dispatching period, which brings frequent data transmission. For example, in Jiangsu Province, China, and Pennsylvania-Jersey-Maryland (PJM) Power Pool, USA [18], the operation data of units are required to be transmitted to the ISO in each minute for guaranteeing the real-time regulation accuracy.

(2) *Explosive data volume*: For achieving exact regulation of each flexible load, lots of advanced measurement and control devices are deployed in the power system, e.g., smart meters, phase measurement units, and control terminals. These devices monitor and transmit various data, e.g., load power, ambient temperature, cooling capacity of each air conditioner, state of charge of electric vehicles, et al. The increasing measurement devices and data categories result in the explosive data volume and transmission demand.

Multi-source data concurrency and huge data transmission lead to non-neglected communication costs for providing operating reserve. Some practical power systems have taken account of communication costs. For example, according to Australian Energy Market, data communication providers and other network service providers are in charge of communication affairs for transmitting data and instructions to and from control centers of flexible loads [19]. In PJM Power Pool, each asset must be charged to get PJMnet, which is the primary wide-area private network for data communication between ISO and LAs [20]. Furthermore, communication prices are actually varying in different regions and time. For instance, the unit communication traffic prices of different regions for Alibaba Cloud in China range from 0.72 to 0.80 RMB/GB [21]. The prices of Google Cloud's egress vary from 0.01 to 0.15 USD/GB among different regions [22]. According to International Telecommunication Union, there are peak time and off-peak prices for the data traffic, which are valued as temporally dynamic communication prices [23].

Some researches consider the communication networks in the optimization of power systems. For example, Han et al. [24] establish an optimization model for the interaction between the distribution network and mobile network to utilize the flexibility of energy storage resources in base stations. Zhou et al. [25] propose a spatial–temporal energy management scheme for base stations in the cellular network. Yong et al. [26] focus on the dispatch potential of cellular base stations equipped with backup batteries to provide regulation services. Xin et al. [27] assess the cyber-contingencies on the power system based on the information network model. However, the above researches do not consider communication costs in the power system operation. Different reserve requirements and dynamic communication prices can affect the allocation of operating reserve among distributed flexible loads, which may further increase the regulation cost and impact the system balance.

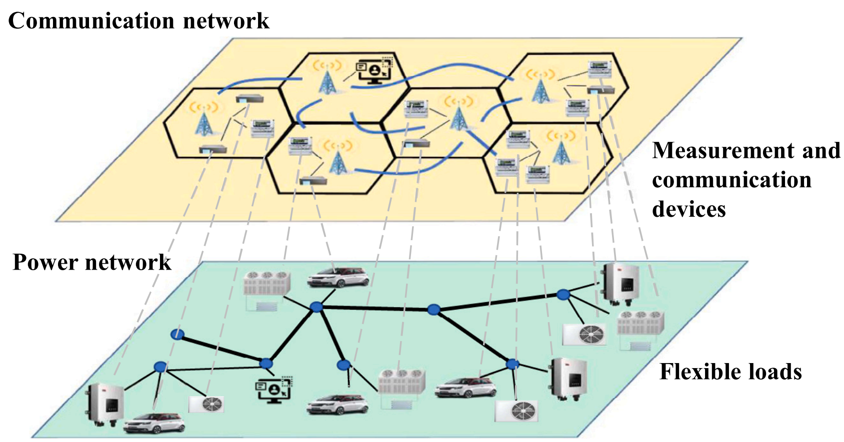

Fig. 1. The system structure of coordinated optimization on power-communication coupling networks for dispatching large-scale flexible loads to provide operating reserve.

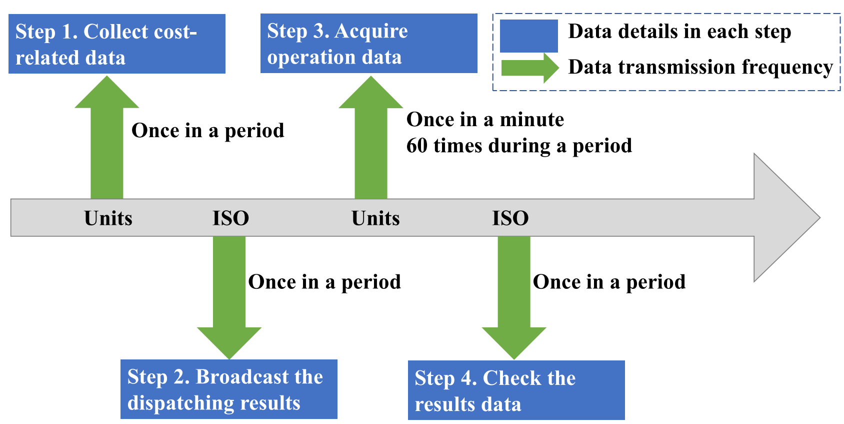

Fig. 2. Data transmission process during a dispatching period (e.g., 1 h) for operating reserve.

1.3. Contributions

To fill the above research gap, this paper proposes a coordinated optimization framework of power-communication coupling networks for dispatching large-scale flexible loads to provide operating reserve. The major contributions are as follows:

(1) We establish a power-communication equivalent model for the optimal dispatching of operating reserve resources, which couples the regulation power and transmitted data from flexible loads. Specifically, the data nodes and branches in the communication network are formulated equivalently with power nodes and branches in the power network.

(2) Based on the power-communication equivalent model, we propose an optimal dispatching scheme of operating reserve resources. In this manner, the power flow and communication flow can be coordinately optimized to minimize the total operation cost by balancing different regulation costs of distributed flexible loads and dynamic costs of communication branches.

(3) We analyze the proposed framework by 5-bus and 118-bus power-communication coupling networks. Numerical results illustrate that the coordinated optimization framework reallocates operating reserve capacities and decreases the regulation cost of power-communication coupling networks.

The rest of this paper is organized as follows. First, the equivalent optimization model for the communication network is established in Section 2. The coordinated optimization model for dispatching operating reserve resources is presented in Section 3. Section 4 illustrates case studies. Section 5 concludes this paper.

2. Equivalently modeling of the communication network to power network

To achieve the coordinated optimization of the power-communication coupling networks, the communication network is established equivalently to the power network, consisting of data nodes, branches, and topology network. Table 1 illustrates the equivalent components and parameters of the power and communication networks, including the node, source, branch, data volume D_i, communication flow D_k^{F}, and communication cost C_k^{F}.

The equivalent items have the exactly physical meanings for the communication network: (*i*) In the power network, ISO dispatches flexible loads to provide operating reserve. Equivalently, the data center in the communication network is in charge of dispatching the data volumes in each branch. (*ii*) Nodes in the power network are electricity buses, while nodes in the communication network are base stations. (*iii*) Power sources involve load aggregators. Correspondingly, data sources come from various measurement units. (*iv*) The injection to each power node is the operating reserve capacities from flexible loads aggregated by LAs, while the injection to each communication node is the data volume from the measurement units. (*v*) The data flow D_k^{F} through the communication branch is equivalent to the power flow P_l^{F} through the power branch. (*vi*) The regulation cost C_i^{P} is related to the regulation power R_i of flexible loads, while the communication cost C_k^{F} is related to the communication flow D_k^{F} in each branch.

2.1. Equivalently modeling of data nodes

Analogous to nodes in the power network (i.e., power sources and power loads), the data nodes are equivalently modeled into two types

Table 1
Equivalent parameters of power and communication networks.

Item	Power network	Symbol	Communication network	Symbol
Network structure	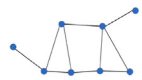	N/A	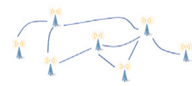	N/A
Operator	ISO	N/A	Data center	N/A
Node	Electricity bus	N/A	Base station	N/A
Source	Load aggregator	N/A	Measurement unit	N/A
Injection	Regulation power	R_i	Data volume	D_i
Branch	Power branch	b	Communication branch	k
Flow	Power flow	P_l^{P}	Communication flow	D_k^{F}
Cost	Regulation cost	C_i^{P}	Communication cost	C_k^{F}

(i.e., data sources and data loads). As shown in Fig. 2, the operation data is transmitted from LAs to ISO during the monitoring process. In the communication network, base stations take charge of LAs' data, respectively. All the data are finally transmitted to the data center collecting LAs' data for the ISO. Thus, base stations with LAs' data are valued as the data sources and the data center is modeled as the data load. For the operating reserve service, there is only one ISO in the power network in charge of the dispatching affairs. Correspondingly, there is only one data load (i.e., the data center node) and several data sources depending on the number of base stations.

The details of the equivalent model for data nodes are as follows.

2.1.1. Modeling of data source nodes

The data volume sent by one LA depends on the number and types of aggregated flexible loads [28]. For instance, the operating reserve capacity of a residential individual is less than that of an industrial individual. If a residential LA prefers to provide the same operating reserve capacity as an industrial LA, the data volume of the residential LA is probably larger than that of the industrial LA. As for one LA, the data volume will relatively grow with the increase of the operating reserve capacity. Therefore, the data-sending volume from a data source node can be modeled as follows [28]:

$$D_i^{\mathrm{S}}(t) = \lambda_i(t) \cdot R_i^{\mathrm{A}}(t), \quad \forall i \in \mathcal{I},\ \forall t \in \mathcal{T}, \tag{1}$$

where $D_i^{\mathrm{S}}(t)$ is the data-sending volume of the ith node at time t; $R_i^{\mathrm{A}}(t)$ is the operating reserve capacity of the LA on the ith node at time t; Symbols $\mathcal{I}$ and $\mathcal{T}$ represent the set of data nodes and time slots, respectively. The parameter $\lambda_i(t)$ represents the relationship between the operating reserve capacity and the data-sending volume for the LA on the ith node at time t. In this paper, flexible loads are utilized by LAs to provide operating reserves. The value of $\lambda_i(t)$ purely varies from different LAs, and satisfies $\lambda_i(t) > 0$. Furthermore, as a discussion, When the LAs provide more than one type of regulation services, the parameter $\lambda_i(t)$ varies with the communication requirements, apart from those for LAs. For example, the data collection frequency for frequency regulation is 30 times in a 5-minute interval, whereas, for operating reserve, it is 5 times within the same interval. This results in the parameter $\lambda_i(t)$ for frequency regulation being six times larger than that for providing operating reserve. For example, the data collection frequency for frequency regulation is 30 times in a 5-minute interval, whereas, for operating reserve, it is 5 times within the same interval. This results in the parameter $\lambda_i(t)$ for frequency regulation being about six times larger than that for providing operating reserve.

2.1.2. Modeling of data load nodes

The ISO and the data center play equivalent roles in the power network and communication network, respectively. In the power network, the ISO takes charge of the system balance between the supply side and the demand side. To maintain the system balance, the regulation resources of LAs with flexible loads are dispatched by the ISO. To support the dispatching process, ISO collects all the operation data from the LAs participating in the operating reserve service. It follows that large volumes of data are transmitted from LAs to the ISO by communication networks during the dispatching process. Thus, equivalently to the ISO, the data center takes charge of the data volume balance by allocating the data traffic from base stations in the communication network. Accordingly, the data center is modeled as the only data load node in the communication network. All the operation data of flexible loads are collected by the ISO. It means that the sum of data-sending volume is equal to the data-receiving volume. Therefore, the data-receiving volume of the data load node is derived as:

$$D_j^{\mathrm{L}}(t) = \sum_{i \in \mathcal{I}, i \neq j} D_i^{\mathrm{S}}(t),\ \forall t \in \mathcal{T}, \tag{2}$$

where $D_j^{\mathrm{L}}(t)$ is the data-receiving volume of the ISO on the jth node at time t.

To specify the relationship between the data center in the communication network and the ISO in the power network, it is worth noting that the data center is a fundamental entity in the communication network that supports the ISO in the power network by gathering operation data from regulation resources. In the power network, the ISO processes the dispatching results, while it does not provide any regulation resources in the power network. The power flows across power branches from one electricity bus to another within the network, rather than flowing into the ISO. In contrast, in the communication network, the data center processes the data traffic allocation problem and simultaneously serves as a data load. It means that the LAs' data will flow from one base station to another and ultimately into the data center. Then, the operation data collected by the data center will be provided to the ISO to check the regulation results.

2.1.3. Categories of data nodes

As described in Fig. 3, there are 4 types of data nodes according to the number of inputs and outputs in the communication networks. Fig. 3(a) indicates a single-input, multiple-output data node. The single input refers to the injected data volume if the node is a data source node. Alternatively, it means the node is the data-receiving node of this directly connected branch. The multiple outputs mean the node is the data-sending node of the other directly connected branches. Fig. 3(b) indicates a multiple-input, multiple-output data node. If the node is a data source node, one of the inputs represents the injected data volume. Alternatively, it signifies that the node is the data-receiving node for all directly connected input branches with the types of inputs. The multiple outputs indicate that the node is the data-sending node of the other directly connected branches. Fig. 3(c) indicates a single-input, single-output data node. The single input represents the injected data volume if the node is a data source node. Alternatively, it means the node is the data-receiving node of this directly connected branch. The single output indicates that the node is the data-sending node of the other directly connected branch. Fig. 3(d) indicates a multiple-input, single-output data node. In the communication network, the data load node is the only node with multiple inputs and a single output simultaneously. The multiple inputs indicate that the data node gathers all the data transmitted within the communication network, which is initially sent

Fig. 3. Four categories of data nodes.

from data source nodes. The single output signifies that the data will be sent to the data center and ultimately utilized by the ISO for dispatching regulation resources in the power network.

2.2. Equivalently modeling of communication branches

A communication branch can be modeled as the data mapping from its data-sending node to its data-receiving node [27]. In this paper, it is assumed that the communication network comprises K data-communication branches for connecting N data nodes.

2.2.1. Modeling of data traffic

Analogous to the power network with the power flow, the data traffic D_k^{F} in the communication branch b_k^{C} is modeled as the communication flow, which is expressed as:

$$D_k^{\mathrm{F}}(t) = \sum_{i \in \mathcal{I}} D_{i,k}^{\mathrm{S}}(t), \quad \forall k \in \mathcal{K},\ \forall t \in \mathcal{T}, \tag{3}$$

where $D_k^{\mathrm{F}}(t)$ is the data traffic (i.e., communication flow) in the kth branch at time t. Variable $D_{i,k}^{\mathrm{S}}(t)$ indicates the data traffic allocated to the kth branch in the communication network from the ith node at time t. Symbol $\mathcal{K}$ represents the set of communication branches.

Similar with the power transmission capacity of each power branch, equivalent constraints are also considered for data traffic limits of communication branches in the network. The communication flow $D_k^{\mathrm{F}}(t)$ at time t should satisfy the following upper and lower bounds:

$$\underline{D_k^{\mathrm{F}}} \le D_k^{\mathrm{F}}(t) \le \overline{D_k^{\mathrm{F}}}, \quad \forall k \in \mathcal{K},\ \forall t \in \mathcal{T}, \tag{4}$$

where $\overline{D_k^{\mathrm{F}}}$ and $\underline{D_k^{\mathrm{F}}}$ are the upper bound and lower data traffic bound of the kth communication branch, respectively.

2.2.2. Modeling of communication cost

According to the communication charging scheme by Alibaba Cloud [21], the communication flow can be charged according to the communication price and data traffic, which is derived as:

$$c_k^{\mathrm{F}}(t) = p_k^{\mathrm{F}}(t) \cdot D_k^{\mathrm{F}}(t), \quad \forall k \in \mathcal{K},\ \forall t \in \mathcal{T}, \tag{5}$$

where $p_k^{\mathrm{F}}(t)$ is the communication price function of the kth communication branch at time t, satisfying:

$$p_k^{\mathrm{F}}(t) = a_k(t) \cdot D_k^{\mathrm{F}}(t) + b_k(t), \quad \forall k \in \mathcal{K},\ \forall t \in \mathcal{T}, \tag{6}$$

where $a_k(t)$ and $b_k(t)$ are the communication price parameters of the kth communication branch at time t. Thus, the communication cost function of the kth branch at time t can be transformed into the following quadratic function:

$$c_k^{\mathrm{F}}(t) = a_k(t) \cdot [D_k^{\mathrm{F}}(t)]^2 + b_k(t) \cdot D_k^{\mathrm{F}}(t), \quad \forall k \in \mathcal{K},\ \forall t \in \mathcal{T}. \tag{7}$$

2.3. Equivalently modeling of the communication network

To present the equivalence of the communication network to the power network, the relationship between data traffic and regulation power needs to be clarified:

(1) The data-sending and data-receiving volumes from data nodes in the communication network, generated by dispatching the regulation power of LAs, are equivalent to the power supply and power demand in the power network. In the power network, regulation power comes from LAs with flexible loads. Equivalently, in the communication network, data traffic is generated by dispatching LAs with flexible loads.

(2) The data traffic by communication branches in the communication network is an equivalent element to the power flow in the power network, which is defined by the communication flow. In the power branch, the power flows from one electricity bus to another to maintain the system balance between the supply side and the demand side. Equivalently, in the communication network, data traffic flows by communication branches from one base station to another and ultimately flows into the data center.

Similar with the power network, there are several communication flow constraints in the communication network. According to Kirchhoff's law, the data traffic flowing into a data node equals the traffic that flows out of the data node for each data node.

During the monitoring process, ISO collects the operation data from all the LAs. It means that the data load node is the only multi-input node in the communication network. Thus, the correspondingly nodal balance of communication flow should be satisfied as:

$$\sum_{k \in \mathcal{K}_j} D_k^{\mathrm{F}}(t) = D_j^{\mathrm{L}}(t), \quad \forall t \in \mathcal{T}, \tag{8}$$

where $\mathcal{K}_j$ is the set of communication branches in which the jth node is the data-receiving node. The symbol $D_j^{\mathrm{L}}(t)$ is the data-receiving volume for the ISO node at time t, i.e., data demand in the communication network similar with the load demand in the power network.

Moreover, the other nodes, which are not the data load node, are divided into four types, including multi-output and multi-input nodes, multi-output and single-input nodes, single-output and multi-input nodes, and single-output and single-input nodes. According to the nodal balance of the communication flow, the data traffic balance for those nodes can be defined as:

$$\sum_{k \in \mathcal{K}_i^{\mathrm{RN}}} D_k^{\mathrm{F}}(t) + D_i^{\mathrm{S}}(t) = \sum_{k \in \mathcal{K}_i^{\mathrm{SN}}} D_k^{\mathrm{F}}(t), \quad \forall i \in \mathcal{I},\ \forall t \in \mathcal{T}, \tag{9}$$

where $D_k^{\mathrm{F}}(t)$ is the communication flow in the kth branch at time t. The variable $D_i^{\mathrm{S}}(t)$ is the data-input traffic of the ith node at time t. The symbol $\mathcal{K}_i^{\mathrm{RN}}$ is the set of communication branches in which the ith node is a data-receiving node. The symbol $\mathcal{K}_i^{\mathrm{SN}}$ is the set of communication branches in which the ith node is a data-sending node.

Besides, similar with the source-load balance in the power network, there is an equivalent source-load balance for data traffic in the communication network. Without data loss, all the transmitted data should flow from data source nodes to the only data load node in the communication network. Mathematically, for the data traffic balance in the communication network, the data load should equal the sum of data sources, which is satisfied according to Eq. (2).

3. Coordinated optimization of power-communication coupling networks

3.1. Modeling of the power network

During a dispatching period, generators and LAs increase the generation power or decrease the load power to provide operating reserve. There are several constraints for each unit and the power network.

3.1.1. Power constraints of generators

Generators increase the generation power to provide operating reserve. The dispatched generation power $P_g^{D,G}$ of the generator g is described by:

$$P_g^{D,G}(t) = P_g^{O,G}(t) + R_g^G(t), \quad \forall g \in \mathcal{G},\ \forall t \in \mathcal{T}, \tag{10}$$

$$\underline{P_g^G(t)} \le P_g^{D,G}(t) \le \overline{P_g^G(t)}, \quad \forall g \in \mathcal{G},\ \forall t \in \mathcal{T}, \tag{11}$$

$$-R_g^{D,G} \le P_g^{D,G}(t) - P_g^{D,G}(t-1) \le R_g^{D,G}, \quad \forall g \in \mathcal{G},\ \forall t \in \mathcal{T}, \tag{12}$$

where $R_g^G(t)$ is the regulation power of the generator g at time t. The variable $P_g^{O,G}(t)$ is the original generation power of the generator g at time t. Variables $\underline{P_g^G(t)}$ and $\overline{P_g^G(t)}$ are the lower bound and upper bounds of generation power of the generator g at time t, respectively. The symbols $R_g^{D,G}$ is the ramp rate limit of the generator g. The symbol $\mathcal{G}$ represents the set of generators.

Thus, the bounds of the reserve of generators can be derived as follows:

$$\underline{P_g^G(t)} - P_g^{O,G}(t) \le R_g^G(t) \le \overline{P_g^G(t)} - P_g^{O,G}(t), \tag{13}$$

where $\underline{P_g^G(t)} - P_g^{O,G}(t)$ and $\overline{P_g^G(t)} - P_g^{O,G}(t)$ are the lower bound and the upper bound of generators' reserve, respectively.

3.1.2. Power constraints of LAs

In contrast to generators, LAs decrease the load power to provide operating reserve. The dispatched load power $P_a^{D,A}$ of LA a is represented by:

$$P_a^{D,A}(t) = P_a^{O,A}(t) - R_a^A(t), \quad \forall a \in \mathcal{A},\ \forall t \in \mathcal{T}, \tag{14}$$

$$\underline{P_a^A(t)} \le P_a^{D,A} \le \overline{P_a^A(t)}, \quad \forall a \in \mathcal{A},\ \forall t \in \mathcal{T}, \tag{15}$$

$$-R_a^{D,A} \le P_a^{D,A}(t) - P_a^{D,A}(t-1) \le R_a^{D,A}, \quad \forall a \in \mathcal{A},\ \forall t \in \mathcal{T}, \tag{16}$$

where $R_a^A(t)$ is the load reduction of the LA a at time t. The variable $P_a^{O,A}(t)$ is the baseline of the LA a at time t. Variables $\underline{P_a^A(t)}$ and $\overline{P_a^A(t)}$ are the lower bound and upper bounds of load power of the LA a at time t, respectively. The symbols $R_a^{D,A}$ is the limit of the ramp rate of the LA a. The symbol $\mathcal{A}$ represents the set of LAs.

Thus, the bounds of the reserve of LAs can be derived as follows:

$$P_a^{O,A}(t) - \overline{P_a^A(t)} \le R_a^A(t) \le P_a^{O,A}(t) - \underline{P_a^A(t)}, \tag{17}$$

where $P_a^{O,A}(t) - \overline{P_a^A(t)}$ and $P_a^{O,A}(t) - \underline{P_a^A(t)}$ are the lower bound and the upper bound of LAs' reserve, respectively.

3.1.3. Nodal power balance constraints

In the power network, the power balance for each node should be enforced by constraints as follows:

$$\sum_{g\in\mathcal{M}_m^G} P_g^{D,G}(t) - \sum_{a\in\mathcal{M}_m^A} P_a^{D,A}(t) - \sum_{l\in\mathcal{L}_m} P_l^P(t) = 0, \ \forall t \in \mathcal{T}, \tag{18}$$

where $\mathcal{M}_m^G$ is the set of generators located at the mth node. The symbol $\mathcal{M}_m^A$ is the set of LAs located at the mth node. The symbol $\mathcal{L}_m$ represents the set of power branches directly connected with the mth node. The variable $P_l^P(t)$ is the power flow in the lth power branch, and $\sum_{l\in\mathcal{L}_m} P_l^P(t)$ indicates the net output power flow at the mth node at time t. The symbol $\mathcal{M}$ represents the set of power nodes.

3.1.4. Power flow constraints

The power network constraints are represented by DC power flow [29]. We adopt the industry-calibrated DC power flow to increase the compatibility with the current ISO's practice [30].

$$P_l^P(t) = B_l\left[\delta_m(t) - \delta_n(t)\right], \quad \forall l \in \mathcal{L},\ \forall m,n \in \mathcal{M},\ \forall t \in \mathcal{T}, \tag{19}$$

$$\underline{\delta} \le \delta_m(t) \le \overline{\delta}, \quad \forall m \in \mathcal{M},\ \forall t \in \mathcal{T}, \tag{20}$$

where $P_l^P(t)$ is the power flow in the lth power branch between the mth node and nth node at time t. Variables $\delta_m(t)$ and $\delta_n(t)$ are the bus angles at time t, respectively. Symbols $\underline{\delta}$ and $\overline{\delta}$ are the lower and upper bound of bus angles. The reference bus angle $\delta_m(t)$ is fixed to zero at time t. The symbol $\mathcal{L}$ represents the set of power branches.

3.1.5. Transmission capacity constraints

The transmission capacity constraints for power branches are derived by:

$$\underline{P_l^P(t)} \le P_l^P(t) \le \overline{P_l^P(t)}, \quad \forall l \in \mathcal{L},\ \forall t \in \mathcal{T}, \tag{21}$$

where $\underline{P_l^P(t)}$ and $\overline{P_l^P(t)}$ are the lower bounds and upper bounds of the lth power branch at time t, respectively.

3.2. Coordinated optimization problem

Fig. 4 shows the coordinated optimization problem with spatially coupling networks and temporally varying conditions. Spatially, dynamic communication prices are distributed in the coupling networks with various dispersed flexible loads. Temporally, the regulation demands and dynamic communication prices are varying in the coupling networks. Thus, to study the communication network's impact on the dispatching of reserve resources in the power network, we establish the coordinated optimization model by considering the dynamic characteristic of the communication network spatially and temporally. The objective for operating reserve is to minimize the total regulation cost, which consists of the operating reserve cost of generators and LAs:

$$\min C^{ISO} = C^G + C^P + C^F, \tag{22}$$

where C^{ISO} is the total regulation cost. The symbols C^G and C^P represent the regulation cost of generators and LAs, respectively. The symbol C^F is the communication cost. The generator's regulation cost is expressed as:

$$C^G = \sum_{t\in\mathcal{T}}\sum_{g\in\mathcal{G}} c_g^G\left[R_g^G(t)\right], \tag{23}$$

where c_g^G is the regulation cost function of generators, which varies with different generators and different operating reserve capacities R_g^G. The quadratic function is generally formulated to represent the regulation cost of generators [31], satisfying $c_g^G = \alpha_g^G \cdot \left[R_g^G(t)\right]^2 + \beta_g^G \cdot R_g^G(t)$.

The load regulation cost and communication cost for LAs can be expressed as:

$$C^P = \sum_{t\in\mathcal{T}}\sum_{a\in\mathcal{A}} c_a^P\left[R_a^A(t)\right], \tag{24}$$

$$C^F = \sum_{t\in\mathcal{T}}\sum_{k\in\mathcal{K}} c_k^F\left[D_k^F(t)\right], \tag{25}$$

where c_a^P is the operating reserve cost function of the LA a with respect to its operating reserve capacity $R_a^A(t)$. The quadratic function is assumed to represent the load reduction cost of LAs [31], satisfying $c_a^P = \alpha_a^A \cdot \left[R_a^A(t)\right]^2 + \beta_a^A \cdot R_a^A(t)$. The variable c_k^F is the communication cost function according to Eqs. (5)–(7).

Based on the above optimization objective in Eqs. (22)–(25), the communication network constraints in Eqs. (1)–(9), and the power network constraints in Eqs. (10)–(21), the operating reserve resources from generators and LAs can be optimally allocated for minimizing the total system regulation cost.

The objective function (22) is a quadratic function, in which all the quadratic terms are positive and no cross terms. Therefore, the Hessian matrix $H(t)$ during the tth period is a diagonal matrix, which is derived by:

$$H(t) = diag[2\alpha_1^G(t), \ldots, 2\alpha_g^G(t), \ldots, 2\alpha_G^G(t), \tag{26}$$

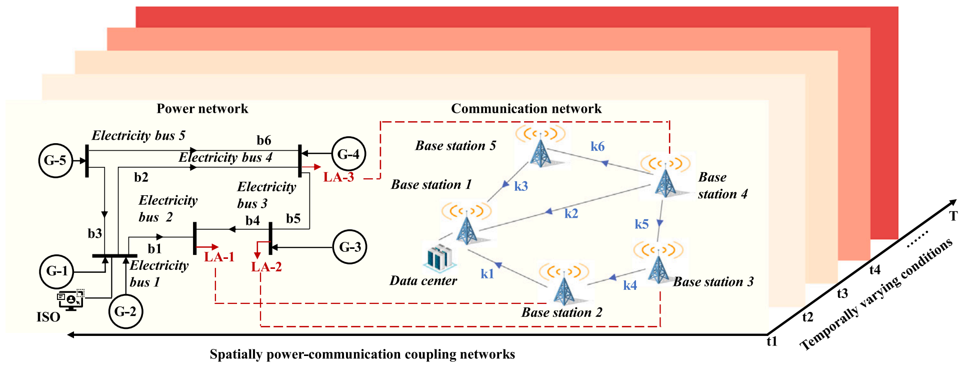

Fig. 4. The coordinated optimization problem with spatially coupling networks and temporally varying conditions.

$$2\alpha_1^A(t), \ldots, 2\alpha_a^A(t), \ldots, 2\alpha_A^A(t),$$
$$2a_1(t), \ldots, 2a_k(t), \ldots, 2a_K(t)],$$

where all the elements are positive at time t. Thereby, the Hessian matrix in Eq. (26) is positive definite. Besides, all the constraints in the model are affine functions. Therefore, the optimization problem is a convex quadratic programming problem and has a unique optimal solution [32]. This proposed model can be efficiently solved using commercial solvers such as CPLEX and GUROBI [33].

4. Case studies

In this section, we conduct two test cases to validate the proposed coordinated optimization framework of power-communication coupling networks. The first one is a small-scale case, which consists of 5-bus power and communication coupling networks based on the typical IEEE 5-Bus Test System. The second one is a large-scale case based on IEEE 118-Bus Test System. To focus on the impact of the dynamic communication network on the power network, we assume that the communication network is the private network purely reserved for dispatching regulation resources in power systems.

The parameters of the 5-bus case are set as follows: (i) The topology of IEEE 5-Bus Test System is described by Fig. 4. The total capacity is 1330 MW with five generators in the power network. And the ISO is located at the 1-st node. It is assumed that the operating reserve requirement is 200 MW at 12:00–13:00 pm. (ii) The communication price for each communication branch is referred to the communication service scheme of Alibaba Cloud and Google Cloud [21,22]. (iii) There are three LAs in the 5-bus coupling network. As described in Table 2, each LA aggregates different types and numbers of load individuals. The average number of data measurement units equipped for one load individual varies in each LA. Furthermore, the parameter λ is assumed. Based on the historical data [28,34], LA-1 decreases its aggregation load power by 3520 MW with 896 GB of the operation data volume transmitted during the monitoring process. LA-2 decreases the aggregation load power by 1887 MW with 304 GB of the operation data volume transmitted during the monitoring process. And LA-3 decreases the aggregation load power by 3520 MW with 982 GB of the operation data volume transmitted during the monitoring process. The effectiveness of the proposed framework is validated based on the following two schemes:

S1: In the traditional scheme, there are no communication charging rules for dispatching large-scale flexible loads, while the communication cost is actually existed.

S2: In the proposed scheme, the coordinated optimization model is implemented by balancing power regulation costs and communication costs.

The proposed models and methods are formulated in MATLAB R2022a, and solved by GUROBI [35] 9.5.2 on a desktop computer with Intel(R) Core(TM) i7-10700 CPU, clocking at 2.90 GHz and 16 GB RAM.

Table 2
The composition of each LA in the 5-bus test system.

	Industrial loads	Commercial loads	Residential loads	Average number of measurement units
LA-1	48	95	20	20
LA-2	63	6	0	16
LA-3	32	190	40	13

4.1. Optimization results of the IEEE 5-Bus test system

The dynamic communication prices are spatially distributed in the coupling networks. By considering the impact of the communication network, each unit's operating reserve capacity is reallocated in S2 compared with S1. Fig. 5 presents the deployed generation power and load power in S1 and S2. Fig. 6 shows the change of their operating reserve capacities in S1 and S2.

The total operating reserve capacity from generators increases in S2 compared with S1 while the reserve capacity of LAs decreases. Table 3 lists the original generation power, deployed power and the reserve capacity of G-3 and G-4, respectively. We can see that the original generation power of G-3 and G-4 are 323.49 MW and 0 MW, respectively. Thus, G-4 increases its generation power by 104.16% from 3.98 MW to 8.13 MW, and also increases the reserve capacity by 104.16%. By contrast, G-3 increases its generation power by 0.58% from 326.14 MW to 328.05 MW, and increases the reserve capacity by 71.60% from 2.65 MW to 4.56 MW. Generators G-1 and G-2 are working on the maximum generation power, and have no operating reserve capacities. And the operating reserve capacity of the generator G-5 is zero since it is dispatched as the original generation power. In contrast, the total operating reserve capacity from LAs decreases from 193.36 MW in S1 to 187.31 MW in S2 because of the communication costs for dispatching large-scale distributed flexible loads. Impacted by different branches' communication prices, the LA-3's operating reserve capacity decreases by 27.43%, while the operating reserve capacities of LA-1 and LA-2 increase by 74.53% and 102.57%, respectively.

With the changes of each unit's allocated operating reserve capacity, the data volume from each data source node accordingly changes, as described in Fig. 5. Compared with S1, the data volumes in S2 from base stations 2 and 3 increase by 74.53% and 102.57%, respectively. The data volumes from base stations 1 and 4 decrease by 9.33% and 27.43%, respectively. The changing rates of each data source node in the communication network are in one-to-one correspondence with the operating reserve capacity of each LA in the power network. Furthermore, the communication flow and power flow have to be rearranged to minimize the total cost. The communication flows in the communication branches k3 and k6 increase from 0 GB to 9.49 GB. However, the communication flow in the communication branch k2 decreases by 49.60% under the impact of high communication prices. In addition, the power flows in b1 and b3 decrease by 6.38% and 3.11%,

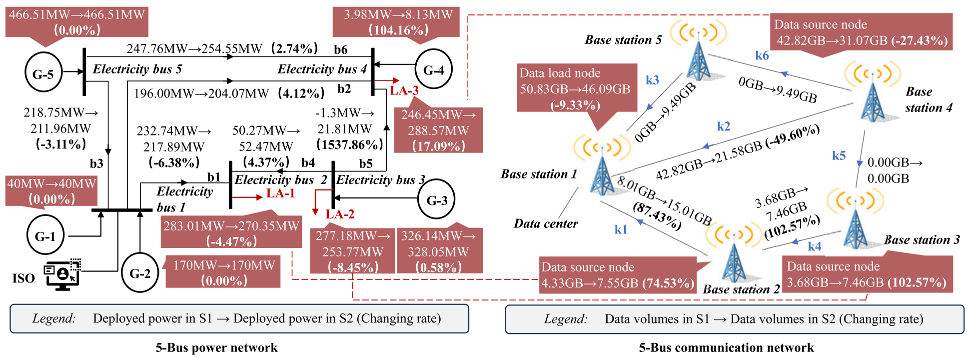

Fig. 5. The power flow and communication flow in the 5-bus power-communication coupling networks.

Table 3
Dispatching results of G-3 and G-4.

	Original power	Deployed power in S1	Deployed power in S2	Changing rate	Reserve capacity in S1 (Original power-Deployed power in S1)	Reserve capacity in S2 (Original power-Deployed power in S2)	Changing rate
G-3	323.49	326.14	328.05	0.58%	2.65	4.56	71.60%
G-4	0	3.98	8.13	104.16%	3.98	8.13	104.16%

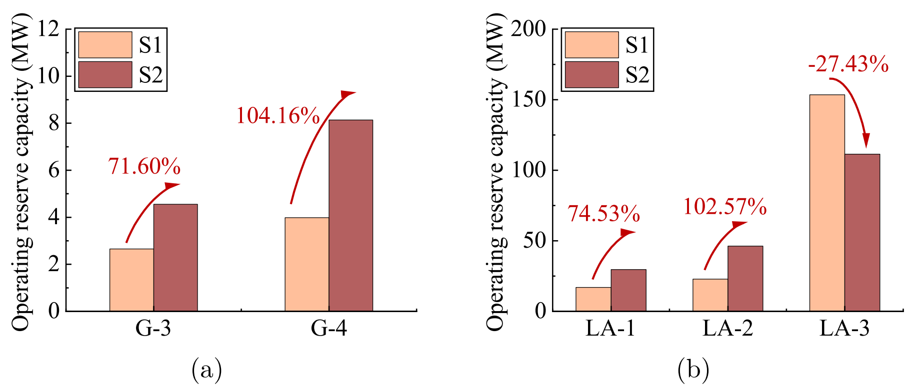

Fig. 6. Operating reserve capacity of generators and LAs in S1 and S2: (a) generators; (b) LAs.

Table 4
Optimized operation costs of the IEEE 5-Bus Test System.

Items	S1 ($)	S2 ($)
GUs' regulation cost	80.96	162.95
LAs' regulation cost	2760.85	2260.09
Communication cost	449.00	234.27
Total regulation cost	2841.81	2657.31

respectively, while the other four branches' power flows increase. To sum up, the rearrangement of communication flow and power flow validates it is worth to consider communication costs for dispatching large-scale flexible loads.

Table 4 describes the cost reduction in S2 compared with S1. The most obvious change is that the proportion of the communication cost to the total regulation cost decreases by 44.20% from 449.00$ to 234.27$. The total cost of the operating reserve service decreases by 6.49% from 2841.81$ to 2657.31$. The results illustrate the effectiveness of the proposed coordinated optimization framework of power-communication coupling networks.

4.2. Analysis on communication networks

(1) The impact of communication limitations on the communication network

Furthermore, we study the impact of communication limitations on the communication network. Fig. 7 describes the communication flows in communication branches in S2 and S3. In S2, there is no congestion in the communication network. However, when congestion occurs in branch k2 in the communication network (S3), the communication flow in branch k2 decreases by 30.49% from 21.58 GB to 15 GB constrained by k2's communication capability. Simultaneously, communication flows are transferred to other branches, i.e., k1, k3, k4, k5, and k6. Especially for branch k5, the communication flow increases from 0. It is utilized to transfer the extra data traffic due to the congestion of branch k2.

Then, we analyze the different data transmission situations in the communication network in Fig. 8. Sometimes the data can be passed directly to the data center. For example, base station 2's data is transmitted by branch k1 to the data center in the 5-bus coupling networks. However, in general, the data may not be passed directly to the data center under the following situations in Fig. 8. In Fig. 8(a), there is no communication branch between base station 3 and the data center. Thus, the data needs to be initially routed to base station 2 and then transferred to the data center. In Fig. 8(b), we take into consideration the limited transmission capability of branch k2, which leads to the situation where the original data volume in Fig. 8(a) surpasses the transmission capability of the directly connected communication branch. In other words, congestion arises in branch k2. The excess data of base station 4 needs to be transferred to other branches. In Fig. 8(c), base station 4's data is directly transmitted to the data center

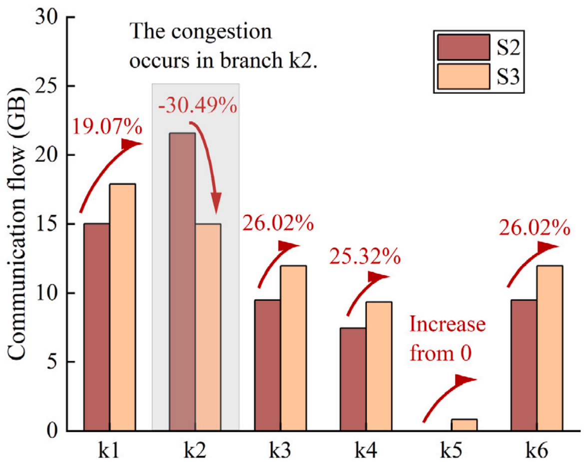

Fig. 7. Communication flows in communication branches in S2 (with no congestion) and S3 (with one-branch congestion).

Table 5
Coordinated optimization results in S2 and S4.

	S2[a]	S4[b]
Generators' regulation capacity (MW)	12.69	15.40
LAs' regulation capacity (MW)	187.31	184.60
Total data volume (GB)	46.09	45.15
Total regulation cost ($)	2657.31	2771.13

[a] Data center is located at base station 1 in S2.
[b] Data center is located at base station 5 in S4.

through branch k2, leading to the communication cost of 231.47$ for a data volume of 31.07 GB. In Fig. 8(d), some of base station 4's data is directly passed to the data center while the rest of the data is transmitted through the other node through branches k6 and k3. By this approach, the communication cost can be reduced by 26.89%, from 231.47$ to 169.24$. Therefore, if the data is transmitted through node after node, the communication cost may decrease due to the spatially dynamic communication prices across the communication network.

(2) The impact of the data center's location on the communication network

In S2, the data center is assumed to be situated at the same location as the ISO in the coupling networks. However, in some systems, the locations of the data center and the ISO may be different. Thus, to study the impact of the location of the data center, another case S4 has been considered in which the data center is located at base station 5. Table 5 compares coordinated optimization results in S4 with S2.

After changing the location of the data center, the ISO reallocates the regulation capacities of generators and LAs. Generators' regulation capacities have an increment of 21.37% while LAs' regulation capacities decrease by 1.45%. It follows that the total data volume decreases by 2.03% in the communication network. Besides, the cost increases by around 4.28% when the data center changes the data center's location from base station 1 to base station 5. It means the change of the data center's location tends to impact the communication flow in the communication network and further leads to the change of dispatching results.

4.3. Sensitivity analysis of communication prices

In this section, we study the sensitivity of communication prices on different branches, so as to find the key communication branch and provide suggestions for channel expansion. Table 6 illustrates the changing rate (CR) of the communication flow in each branch when its communication price changes. For instance, the communication flow in branch k1 decreases 6% when its communication price increases 25%. It can be seen from Table 6 that the communication flow in branch k2 changes most significantly with the changes of communication prices. It means that the communication branch k2 in the coupling networks is important, which can result in a more significant reallocation of the operating reserve resources. Therefore, the key branch identification can help to provide channel expansion suggestions for communication branches and reduce the total regulation cost of flexible loads.

Apart from the impact on communication flow, the communication prices can also affect the operating reserve capacities of generators and LAs. Fig. 9 describes the optimized operating reserve capacities of generators and LAs as the changing communication prices. Here the prices of all the communication branches are assumed to be increased from 0 to 200 times. As we mentioned before, generators G-1 and G-2 have already reached their maximum generation powers. Thus, both of them have no operating reserve capacities. With the increase of communication prices, generators G-3, G-4 and G-5 are dispatched to provided more operating reserve capacities, while the relative rate of change (RoC) gradually slows down. For LAs, LA-1's operating reserve capacity increases as the communication prices grow from 0 to 4 times. Once the communication prices exceed 4 times, the operating reserve capacity tends to decrease. The maximum of LA-1's operating reserve capacity is 35.06 MW. Similarly, LA-2's operating reserve capacity increases as the communication prices grow from 0 to 9.5 times. And then, it tends to decrease. The maximum of LA-2's operating reserve capacity is 72.53 MW. Different from LA-1 and LA-2, LA-3's operating reserve capacity always declines with the increase of communication prices. Nevertheless, although the trend of each LA's operating reserve capacity is different, the total operating reserve capacities of LAs continuously decrease with a higher communication price.

Fig. 10 shows the power regulation and communication costs of LAs as the communication prices increase from 0 to 200 times. The load reduction cost of LAs in Fig. 10(a) decreases due to the decline of LAs' operating reserve capacities. The communication cost of LAs increases until the communication prices increase by 38 times. After that, the communication cost starts to decline due to the decrease in LAs' operating reserve capacities. In Fig. 10(b), the total cost for providing operating reserve increases with the improvement of communication prices, which illustrates the significant role of the communication network for the power network.

4.4. Optimization results of the IEEE 118-Bus test system

This section illustrates the proposed coordinated optimization scheme based on the IEEE 118-Bus Test System. The parameters are set as follows: (i) The topology of IEEE 118-Bus test system is described by Fig. 11. The system capacity is 9966.20 MW with 54 generators. The power network has 99 LAs aggregating large-scale flexible loads. (ii) It is assumed that the operating reserve requirement accounts for around 20% of the total load in the 118-bus power network. (iii) The peak and off-peak time of the dynamic communication prices is set referred to the Alibaba Cloud, i.e., 08:00–24:00 as peak time and 00:00–08:00 as off-peak time [36].

(1) The impact of spatially different communication prices on dispatching reserve resources

Spatially different communication prices can impact the dispatching results of operating reserve resources, especially considering that large-scale flexible loads are distributed in different nodes. The heat maps in Fig. 11 describe the spatially allocated operating reserve capacity for each unit in the 118-bus power network in one period. Figs. 11(a)–(c) show the dispatching results based on the traditional scheme (S1), while Figs. 11(d)–(f) show the dispatching results based on the proposed coordinated scheme (S2). By comparing Figs. 11(a) and 11(d), the total operating reserve capacity of generators increases after considering the communication costs. Specifically, the third top unit of the operating reserve capacity among all the generators changes

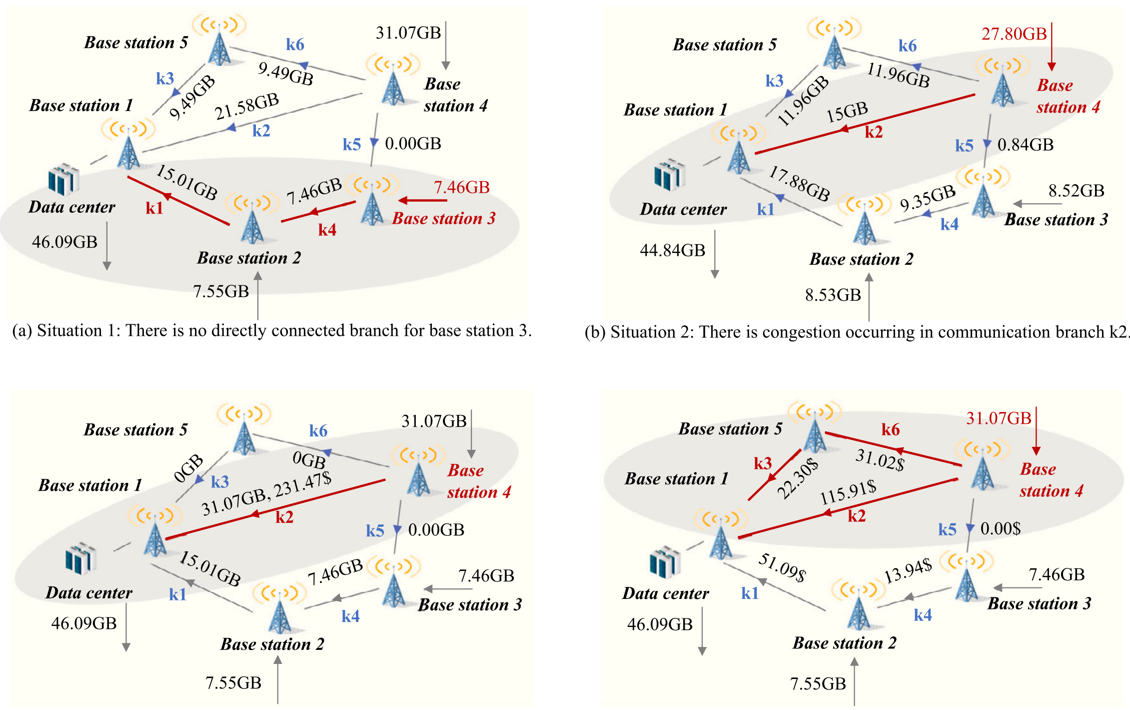

(a) Situation 1: There is no directly connected branch for base station 3.

(b) Situation 2: There is congestion occurring in communication branch k2.

Fig. 8. Different data transmission situations in the communication network.

Table 6
Changing rate (CR) of communication branch flow with prices.

b[1] \ p_k^F [2]	−50% D^F (GB)	CR	−25% D^F (GB)	CR	0% D^F (GB)	25% D^F (GB)	CR	50% D^F (GB)	CR
k1	−18.20	21.24%	−16.44	9.50%	−15.01	−14.10	−6.11%	−13.02	−13.27%
k2	−30.24	40.14%	−25.18	16.70%	−21.58	−18.79	−12.94%	−16.59	−23.12%
k3	−11.51	21.24%	−10.42	9.74%	−9.49	−8.70	−8.36%	−8.01	−15.64%
k4	−8.97	20.27%	−8.13	8.97%	−7.46	−7.21	−3.39%	−6.73	−9.85%
k5	−0.16	N/A	−0.03	N/A	0.00	0.00	0.00%	0.00	0.00%
k6	12.79	34.67%	10.92	14.97%	9.49	8.37	−11.79%	7.47	−21.33%

[1] The symbol b indicates the communication branch.
[2] The symbol p_k^F indicates the communication price of the communication branch.

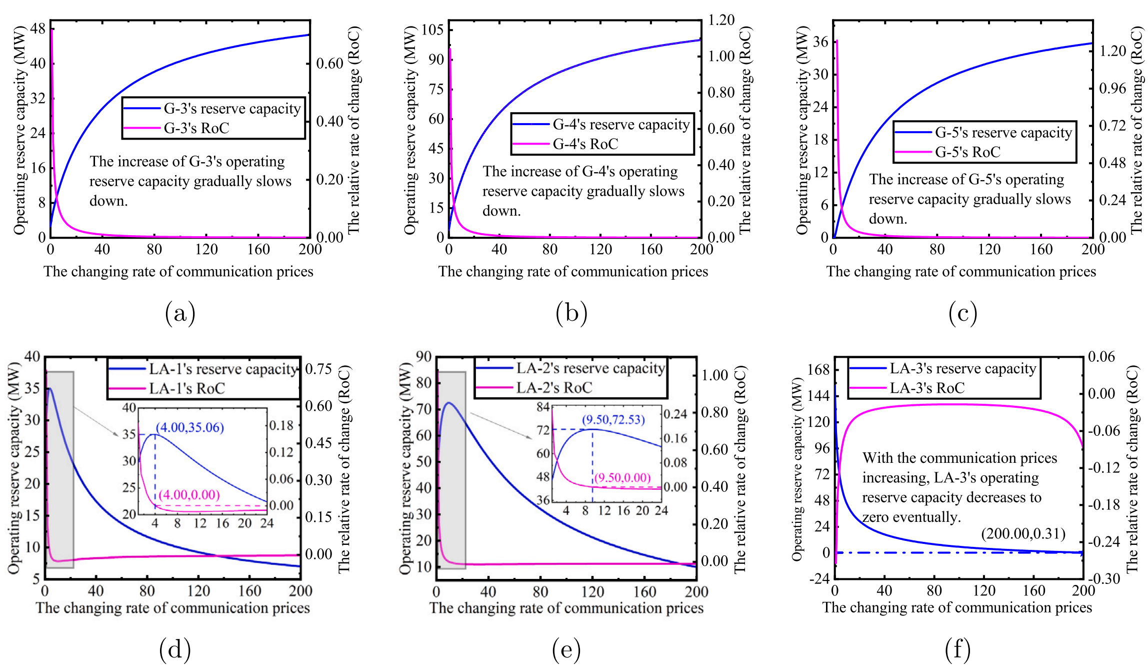

Fig. 9. Sensitivity analysis of units' operating reserve capacities with different communication prices: (a) G-3; (b) G-4; (c) G-5; (d) LA-1; (e) LA-2; (f) LA-3.

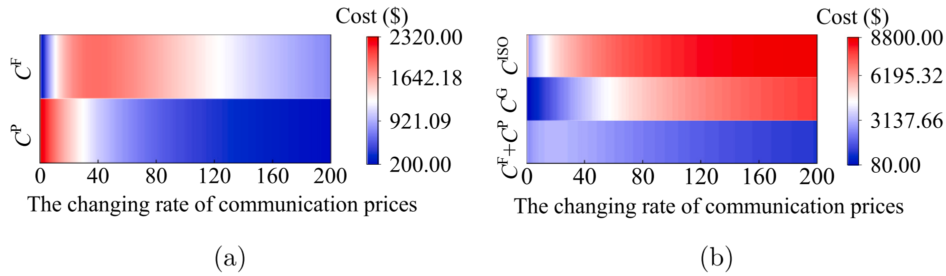

Fig. 10. Sensitivity analysis of communication prices on costs: (a) the power regulation and communication costs of LAs; (b) the regulation costs of generators and LAs.

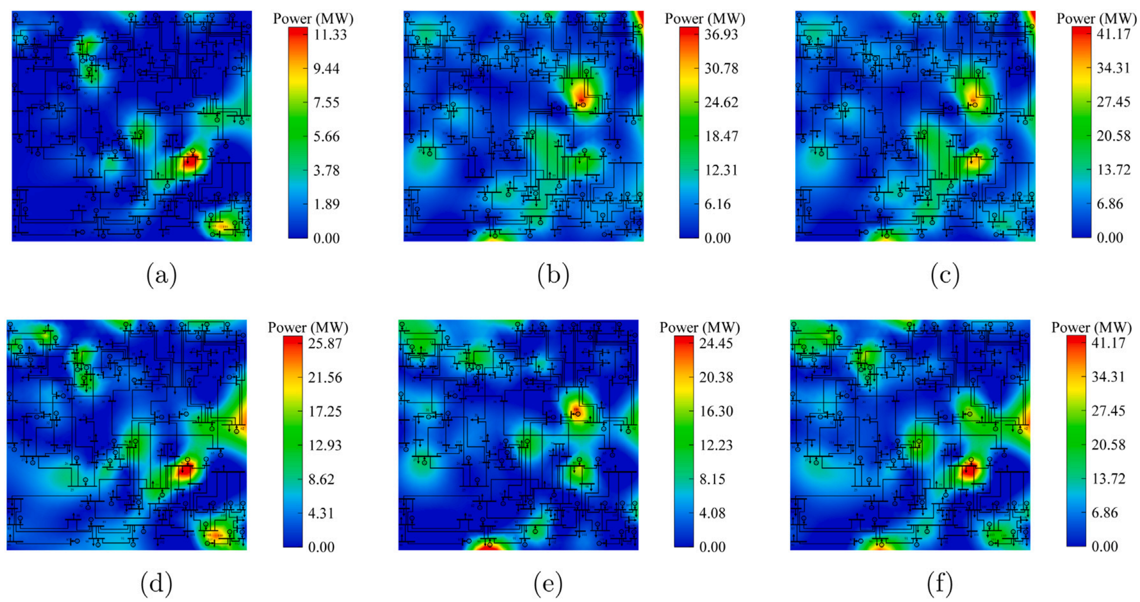

Fig. 11. Operating reserve capacity for each unit in the 118-bus power network in S1 and S2: (a) Generators in S1; (b) LAs in S1; (c) Different nodes in S1; (d) Generators in S2; (e) LAs in S2; (f) Different nodes in S2.

from G-7 at the electricity bus-15 to G-27 at the electricity bus-62. By comparing Figs. 11(b) and 11(e), the total operating reserve capacity of LAs decreases in S2. Specifically, LA-72 at the electricity bus-90 becomes the top of the operating reserve capacity among all the LAs, while LA-51 at the electricity bus-59 has no operating reserve capacity in S2. Considering non-negligible communication costs for dispatching flexible loads, the proposed coordinated optimization scheme reallocates the operating reserve capacities among different nodes, as shown in Figs. 11(c) and 11(f). For example, the operating reserve capacities at electricity bus-15, bus-62, and bus-12 increase significantly, while the operating reserve capacities at electricity bus-59, bus-60, and bus-49 decrease drastically.

(2) The impact of temporally dynamic communication prices on dispatching reserve resources

Apart from the spatial impacts, temporally varying conditions (i.e., temporally dynamic communication prices and temporally different operating reserve requirements) can also impact the dispatching results. Fig. 12 presents the operating reserve requirements of the power network and the average prices of the communication network during 24-hour periods. Fig. 13 describes the dispatching results of G-7, G-37, LA-1, and LA-59 in the coupling networks, which vary temporally in 24-hour periods. The shadow areas in Figs. 13(a) and (b) represent the operating reserve capacities of generators in 24-hour periods. Compared with S1, the proposed coordinated optimization scheme in S2 increases the operating reserve capacities of generators. In contrast, the temporal communication prices have different impacts on LAs. For example, in Fig. 13(c), the operating reserve capacity of LA-1 in S2 is

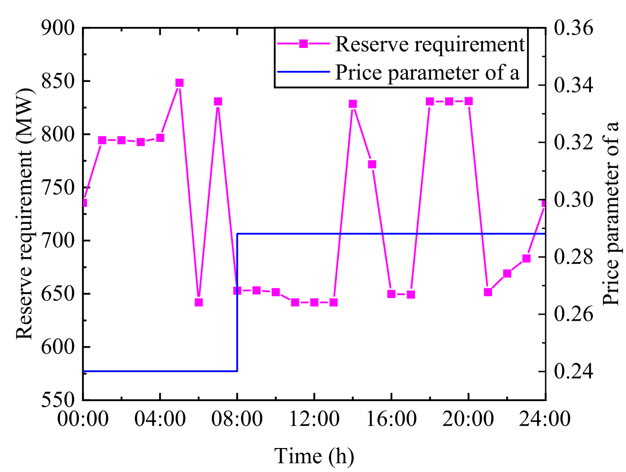

Fig. 12. Reserve requirements and the communication price parameter in the 118-Bus network in one day (24 h).

larger than that in S1, while Fig. 13(d) shows the capacity of LA-59 in S2 is less than that in S1.

Furthermore, temporally varying conditions of communication peak and off-peak prices even lead to non-regulation periods of LAs. During communication off-peak periods from 00:00 to 08:00, the operating reserve capacity of LA-1 in S2 increases by 16.20% from 59.70 MW in S1 to 69.37 MW, while the operating reserve capacity of LA-59 in

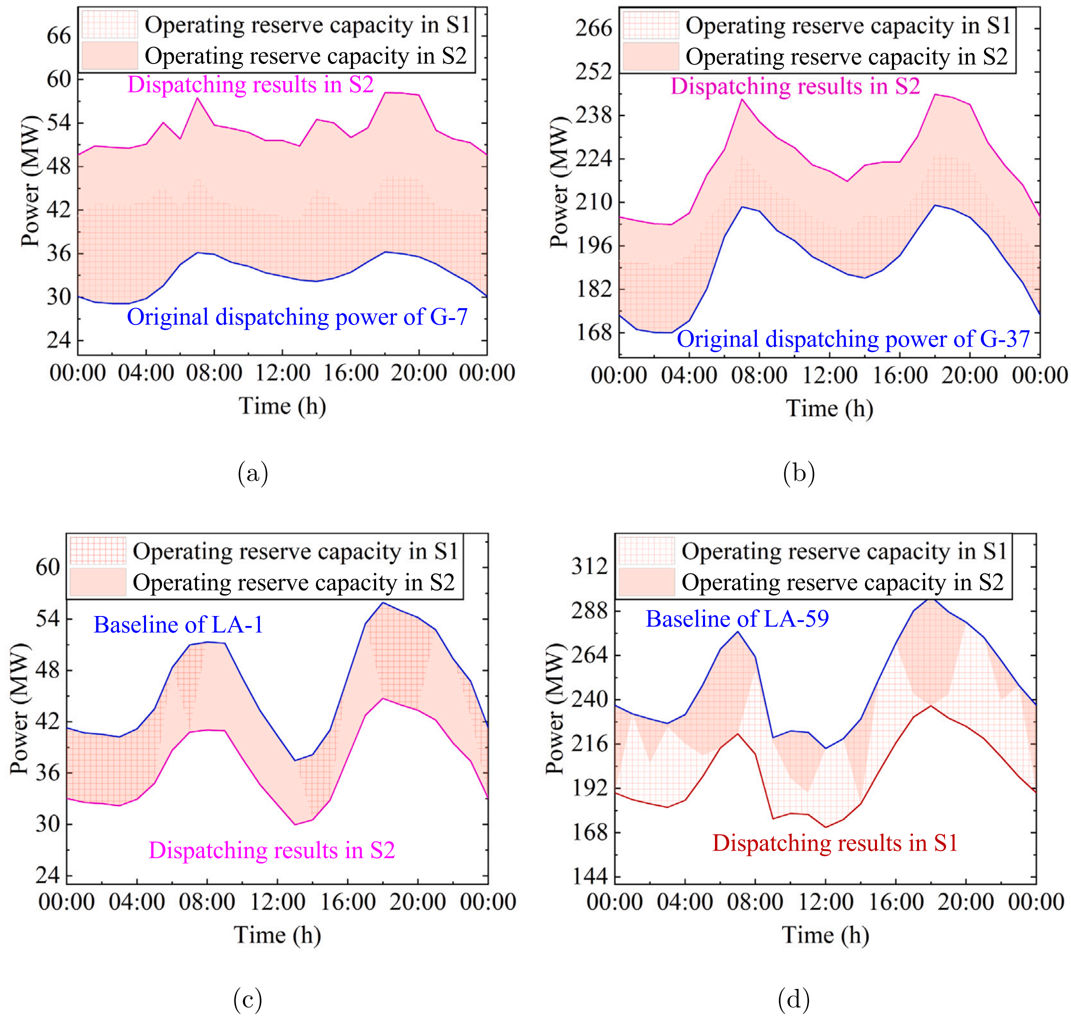

Fig. 13. Reserve requirements and the communication price parameter in the 118-Bus network in one day (24 h): (a) G-7; (b) G-37; (c) LA-1; (d) LA-59.

S2 decreases by 35.60% from 390.09 MW in S1 to 235.64 MW. During communication peak periods from 08:00 to 24:00, the operating reserve capacity of LA-1 in S2 increases by 187.55% from 53.19 MW in S1 to 152.96 MW, while the operating reserve capacity of LA-59 in S2 decreases by 64.86% from 809.62 MW in S1 to 284.48 MW. It can be seen that communication peak prices have a larger impact on the dispatching results of LAs compared with that with communication off-peak prices.

5. Conclusion

In this paper, we propose an optimal framework for allocating operating reserve resources in the power system with large-scale flexible loads considering coupling communication networks. This framework employs: (1) the power-communication equivalent model to formulate the relationship of the components in the power network and communication network; (2) the coordinated optimization model with power flow and communication flow to balance multi-units' regulation costs and dynamic communication costs. Numerical results present the impact of the communication-coupled network on the dispatching of reserve resources with large-scale flexible loads, both spatially and temporally, in the power network, as follows:

(1) By investigating the impact of communication networks, operating reserve capacities among different nodes are reallocated in the power network. Generally, the total operating reserve capacity from generators increases while the capacity of LAs decreases. It follows that the proportion of the communication cost to the total regulation cost decreases by 44.20% and the total cost of the operating reserve service decreases by 6.49%.

(2) The spatially dynamic communication network impacts the communication flows across communication branches due to the various communication prices. Identifying key branches can help provide channel expansion suggestions from communication networks and reduce the total regulation cost of flexible loads.

(3) Temporally dynamic communication prices in the communication network can lead to non-regulation periods of reserve resources. Higher communication prices during peak periods have a larger impact on the dispatching results of reserve resources compared with lower communication prices during off-peak periods.

CRediT authorship contribution statement

Liya Ma: Writing – original draft, Validation, Methodology, Formal analysis, Data curation, Conceptualization. **Hongxun Hui:** Writing – review & editing, Visualization, Project administration, Conceptualization. **Sheng Wang:** Writing – review & editing, Visualization, Software. **Yonghua Song:** Supervision, Resources, Investigation, Funding acquisition.

Declaration of competing interest

The authors declare that they have no known competing financial interests or personal relationships that could have appeared to influence the work reported in this paper.

Data availability

The authors do not have permission to share data.

Acknowledgments

This paper is funded in part by the Science and Technology Development Fund, Macau SAR (File no. 001/2024/SKL, and File no. 0117/2022/A3), in part by the Start-up Research Grant of University of Macau (File no. SRG2023-00063-IOTSC), and in part by the Chair Professor Research Grant of University of Macau (File no. CPG2024-00015-IOTSC).

References

[1] Guo Z, Wei W, Shahidehpour M, Chen L, Mei S. Two-timescale dynamic energy and reserve dispatch with wind power and energy storage. IEEE Trans Sustain Energy 2022;14(1):490–503.
[2] Wang S, Zhai J, Hui H. Optimal energy flow in integrated electricity and gas systems with injection of alternative gas. IEEE Trans Sustain Energy 2023;14(3):1540–57.
[3] Yan L, Chen X, Chen Y, Wen J. A cooperative charging control strategy for electric vehicles based on multiagent deep reinforcement learning. IEEE Trans Ind Inf 2022;18(12):8765–75.
[4] Gan W, Shahidehpour M, Yan M, Guo J, Yao W, Paaso A, et al. Coordinated planning of transportation and electric power networks with the proliferation of electric vehicles. IEEE Trans Smart Grid 2020;11(5):4005–16.
[5] Huang S, Wu Q. Real-time congestion management in distribution networks by flexible demand swap. IEEE Trans Smart Grid 2017;9(5):4346–55.
[6] Lu N. An evaluation of the HVAC load potential for providing load balancing service. IEEE Trans Smart Grid 2012;3(3):1263–70.
[7] Wang S, Hui H, Ding Y, Ye C, Zheng M. Operational reliability evaluation of urban multi-energy systems with equivalent energy storage. IEEE Trans Ind Appl 2023;59(2):2186–201.
[8] Hui H, Siano P, Ding Y, Yu P, Song Y, Zhang H, et al. A transactive energy framework for inverter-based HVAC loads in a real-time local electricity market considering distributed energy resources. IEEE Trans Ind Informat 2022;18(12):8409–21.
[9] Yang S, Lao K-W, Chen Y, Hui H. Resilient distributed control against false data injection attacks for demand response. IEEE Trans Power Syst Early Access, 2023. http://dx.doi.org/10.1109/TPWRS.2023.3287205.
[10] Zhang H, Hu Z, Munsing E, Moura SJ, Song Y. Data-driven chance-constrained regulation capacity offering for distributed energy resources. IEEE Trans Smart Grid 2018;10(3):2713–25.
[11] Wang J, Huang S, Wu D, Lu N. Operating a commercial building HVAC load as a virtual battery through airflow control. IEEE Trans Sustain Energy 2020;12(1):158–68.
[12] Chen X, Hu Q, Shi Q, Quan X, Wu Z, Li F. Residential HVAC aggregation based on risk-averse multi-armed bandit learning for secondary frequency regulation. J Mod Power Syst Clean Energy 2020;8(6):1160–7.
[13] Galli S, Scaglione A, Wang Z. For the grid and through the grid: The role of power line communications in the smart grid. Proc IEEE 2011;99(6):998–1027.
[14] Liang H, Choi BJ, Zhuang W, Shen X. Stability enhancement of decentralized inverter control through wireless communications in microgrids. IEEE Trans Smart Grid 2013;4(1):321–31.
[15] Hui H, Ding Y, Shi Q, Li F, Song Y, Yan J. 5G network-based Internet of Things for demand response in smart grid: A survey on application potential. Appl Energy 2020;257:113972.
[16] Haidar AM, Fakhar A, Muttaqi KM. An effective power dispatch strategy for clustered microgrids while implementing optimal energy management and power sharing control using power line communication. IEEE Trans Ind Appl 2020;56(4):4258–71.
[17] Yang S, Lao K-W, Hui H, Chen Y, Dai N. Real-time harmonic contribution evaluation considering multiple dynamic customers. CSEE J Power Energy Syst 2023. http://dx.doi.org/10.17775/CSEEJPES.2022.06570.
[18] PJM. PJM manual 11: Energy & ancillary services market operations. 2023, [Online]. Available: https://www.pjm.com/directory/manuals/m11/index.html#about.html.
[19] AEMO. Review of power system data communication standard. 2023, [Online]. Available: https://aemo.com.au/consultations/current-and-closed-consultations/review-of-power-system-data-communication-standard.
[20] PJM. Metering system and communication requirements. 2017, [Online]. Available: https://www.pjm.com/-/media/committees-groups/committees/mic/20170620-special/20170620-item-05-der-telemetry-metering-and-communication-requirements.ashx.
[21] Alibaba Cloud. Primary traffic-based billing scheme. 2023, [Online]. Available: https://help.aliyun.com/document_detail/437187.html.
[22] Google Cloud. All networking pricing. 2023, [Online]. Available: https://cloud.google.com/vpc/network-pricing.
[23] International Telecommunication Union. Handbook for the collection of administrative data on telecommunications. Tech. rep., 2020, [Online]. Available: https://www.itu.int/en/ITU-D/Statistics/Pages/publications/handbook.aspx.
[24] Han J, Liu N, Catalão JP. Optimization of distribution network and mobile network with interactive balance of flexibility and power. IEEE Trans Power Syst 2022;38(3):2512–24.
[25] Zhou C, Feng C, Wang Y. Spatial–temporal energy management of base stations in cellular networks. IEEE Internet Things J 2021;9(13):10588–99.
[26] Yong P, Zhang N, Liu Y, Hou Q, Li Y, Kang C. Exploring the cellular base station dispatch potential towards power system frequency regulation. IEEE Trans Power Syst 2021;37(1):820–3.
[27] Xin S, Guo Q, Sun H, Zhang B, Wang J, Chen C. Cyber-physical modeling and cyber-contingency assessment of hierarchical control systems. IEEE Trans Smart Grid 2015;6(5):2375–85.
[28] PJM. Hourly load: Metered. 2023, [Online]. Available: https://dataminer2.pjm.com/feed/hrl_load_metered.
[29] He Y, Yan M, Shahidehpour M, Li Z, Guo C, Wu L, et al. Decentralized optimization of multi-area electricity-natural gas flows based on cone reformulation. IEEE Trans Power Syst 2018;33(4):4531–42.
[30] Yin S, Wang J. Distributionally robust decentralized scheduling between the transmission market and local energy hubs. IEEE Trans Power Syst 2023;38(2):1845–56.
[31] Shen Y, Wu W, Wang B, Sun S. Optimal allocation of virtual inertia and droop control for renewable energy in stochastic look-ahead power dispatch. IEEE Trans Sustain Energy 2023;14(3):1881–94.
[32] Huang S, Wu Q, Oren SS, Li R, Liu Z. Distribution locational marginal pricing through quadratic programming for congestion management in distribution networks. IEEE Trans Power Syst 2014;30(4):2170–8.
[33] Xu Y, Dong ZY, Zhang R, Hill DJ. Multi-timescale coordinated voltage/var control of high renewable-penetrated distribution systems. IEEE Trans Power Syst 2017;32(6):4398–408.
[34] Hui H, Ding Y, Luan K, Chen T, Song Y, Rahman S. Coupon-based demand response for consumers facing flat-rate retail pricing. CSEE J Power Energy Syst Early Access 2023. http://dx.doi.org/10.17775/CSEEJPES.2021.05140.
[35] Gurobi optimization L. Gurobi optimizer Reference manual. 2023, [Online]. Available: https://www.gurobi.com/.
[36] Alibaba Cloud. OSS off-net data traffic charging scheme for different periods. 2023, [Online]. Available: https://help.aliyun.com/noticelist/articleid/6571464.html.